

THE EFFECT OF PHOSPHOLIPID SPECIES ON NON-IDEAL
BEHAVIOR IN CHOLESTEROL-CONTAINING BILAYERS

By RULONG MA

A thesis submitted to the

Graduate School-Camden

Rutgers, The State University of New Jersey

In partial fulfillment of the requirements

For the degree of Master of Science

Graduate Program in Computational & Integrative Biology

Written under the direction of

Grace Brannigan

And approved by

Grace Brannigan

Eric Klein

Guillaume Lamoureux

Camden, New Jersey

October 2019

ABSTRACT OF THE DISSERTATION

THE EFFECT OF PHOSPHOLIPID SPECIES ON NON-IDEAL
BEHAVIOR IN CHOLESTEROL-CONTAINING BILAYERS

By RULONG MA

Dissertation Director:

Grace Brannigan

Cholesterol plays an essential role in membrane properties, such as viscoelasticity and phase separation. However, the effects of phospholipid species on cholesterol in bilayer were not well studied. Here, we study the effects of phospholipids on cholesterol in the bilayer by calculating average lipid lateral area, cholesterol bulk/gas partition coefficient and cholesterol free energy using Alchemical Free Energy Perturbation by decoupling in molecular dynamics simulations. We found that the larger headgroups of the phospholipids, the higher energy of removing cholesterol from the bilayer. Cholesterol has a more substantial bulk/gas partition coefficient in phosphatidylcholine (PC) bilayers than phosphatidylethanolamine (PE) bilayers. The longer saturated hydrocarbon chains, the higher energy of removing cholesterol from the bilayer. However, the higher chains' degree of unsaturation, the less free energy of cholesterol in the bilayer. The quadratic mixture model works well for lateral lipid area but the free energy of cholesterol in the bilayer.

Declaration of Authorship

I, RULONG MA, declare that this thesis titled, “THE EFFECT OF PHOSPHOLIPID SPECIES ON NON-IDEAL BEHAVIOR IN CHOLESTEROL-CONTAINING BILAYERS” and the work presented in it are my own. I confirm that:

- This work was done wholly or mainly while in candidature for a research degree at this University.
- Where any part of this thesis has previously been submitted for a degree or any other qualification at this University or any other institution, this has been clearly stated.
- Where I have consulted the published work of others, this is always clearly attributed.
- Where I have quoted from the work of others, the source is always given. With the exception of such quotations, this thesis is entirely my own work.
- I have acknowledged all main sources of help.
- Where the thesis is based on work done by myself jointly with others,
- I have made clear exactly what was done by others and what I have contributed myself.

Signed:

Date:

Acknowledgements

First of all, I want to express my sincere gratitude to my advisor Dr. Grace Brannigan for the support of my Master study. She is patient in explaining the things I do not understand, and she is accommodating to give many suggestions and help in my study and life. There is no doubt that I can not complete a Master study without her help.

Also, I thank the rest of my thesis committee: Dr. Eric Klein and Dr. Guillaume Lamoureux, for their valuable suggestions and indispensable help in my study.

I want to thank my fellow labmates, Ruchi Lohia, Liam Sharp, Kristen Woods, and Dr. Sruthi Murlidaran, for their help in my study and life. Besides, I also thank Pedro Guicardi and Kaitlin Bassi for their suggestions in thesis writing.

Finally, I want to thank my family for their support and encouragement throughout my Master study and my life.

Abstract	ii
-----------------	----

Declaration of Authorship	iii
----------------------------------	-----

Acknowledgements	iv
-------------------------	----

Contents

1 Introduction	1
1.1 Lipid Bilayer	1
1.2 Cholesterol	3
1.3 The models for studying cholesterol	5
2 Methods	9
2.1 Materials	9
2.2 Simulation details	10
2.3 Alchemical free energy Perturbation Calculations	12
3 Results	13
3.1 Effect of phospholipid on condensing effect of cholesterol	13
3.2 Effect of phospholipid on chemical potential of dilute cholesterol	14
3.3 Effect of phospholipid on cholesterol non-ideality	17
4 Discussion	18
5 References	21
6 Supplemental Material	24

1 Introduction

1.1 Lipid Bilayer

A lipid bilayer is composed of a double layer of lipids, arranged with the hydrophobic acyl chains of each layer facing each other, and the hydrophilic head groups on the outside, exposed to water [1]. Almost all biological membranes in all organisms consist of lipid bilayers. Separating aqueous compartments from their surroundings is a significant role of the lipid bilayer. For example, the bilayer forms a continuous barrier around a cell, which separates the interior of all cells from the extracellular space. Moreover, the lipid bilayer provides embedded sites for membrane proteins. The physicochemical properties of biological membranes are mainly determined by the lipid composition, such as membrane fluidity and elasticity [2]. The major lipids in biological membranes are phospholipids (PL), glycolipids, and cholesterol (Chol). Glycerophospholipids, especially phosphatidylcholine (PC) and phosphatidylethanolamine (PE), is the primary structural lipids in eukaryotic membranes [2].

Lipids can self-organize into a bilayer in water because of two main reasons. The lipid bilayer formed when the lipid heads point outwards, and the lipid tails point membrane lipids inwards. The first reason for lipid self-organization is that lipids are amphiphilic molecules. Amphiphilic PL has a hydrophilic head and a hydrophobic tail consisting of one or two hydrocarbon chains (Figure 1). There are three components in the polar head, which are a glycerol backbone, a phosphate, and choline or ethanolamine. The hydrophobic tails are the long hydrocarbon chains with varied carbon number. Lipids aggregate together by headgroup-headgroup contact and tail-tail contact based on polar or nonpolar properties. The predominant

force governing the self-assembly of lipids into bilayers in the aqueous system comes from the hydrophobic effect. The contribution of the hydrophobic effect on a bilayer in water is comparable to a lateral pressure that squeezes the phospholipids together and keeps the nonpolar tails from contacting with water [3].

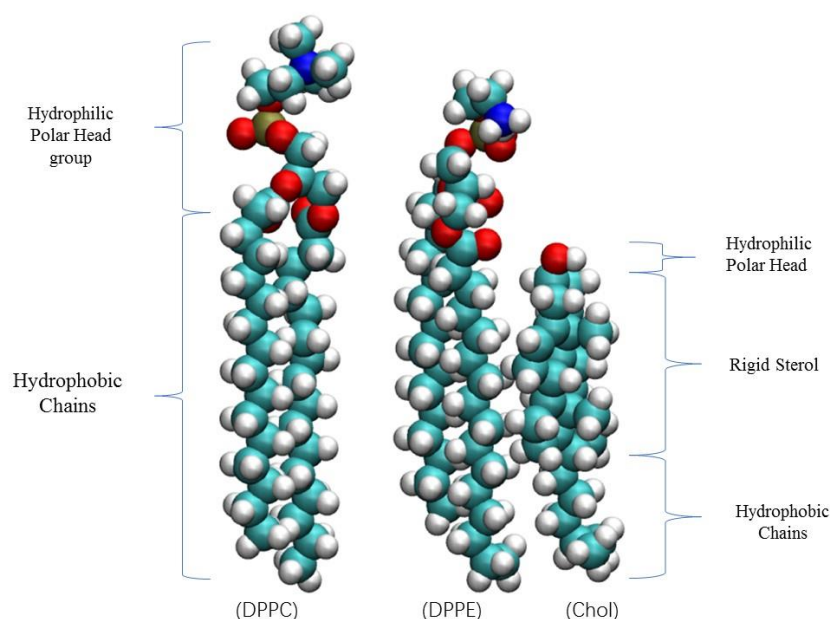


Figure 1. The structure of DPPC, DPPE, and cholesterol. DPPC and DPPE are representatives of PC lipids and PE lipids, respectively. The atoms were presented in different colors. (Carbon: green; Hydrogen: gray; Oxygen: red; Nitrogen: blue; Phosphorus: yellow.)

The lipids are divided into saturated lipids and unsaturated lipids based on the degree of unsaturation of their hydrocarbon chains. There are no double bonds in saturated chains, which tend to be rigid and straight. The unsaturated chains with one or more double bonds tend to be much more flexible [4]. The unsaturated lipids can be grouped into several categories based on the number of double bonds: mono-unsaturated (one double bond), or polyunsaturated fatty acids (PUFA) (with multiple double bonds). A lipid with one saturated hydrocarbon chain and one unsaturated hydrocarbon chain is referred to as a heteroacid.

Unsaturated lipids play an essential role in modulating the membrane fluidity. The unsaturated lipids, especially unsaturated chains with more than one more double bond, have low melting temperatures and tend to be flexible. The lipid packing of a lipid bilayer with unsaturated lipids is loose, and the membrane fluidity is increasing. Moreover, cholesterol, another vital component of the bilayer, can increase lipid mobility [5, 6]. Thus, the cells can modulate the membrane fluidity by changing unsaturation levels of lipids tails and the amount of cholesterol in the membrane [7].

1.2 Cholesterol

Cholesterol is significant for biological membranes. For one thing, cholesterol is required to build and maintain membranes, and the ratio of Chol/PL is high in cell membranes (from 10 to 30 mol% Chol) [2]. The Chol content increases along with the secretory pathway in eukaryotic cell membranes [8]. The condensing effect of cholesterol in the membrane is that the surface area of a cholesterol-containing lipid bilayer is less than the sum of areas of the individual bilayer components [9]. When cholesterol was intercalated into the loosely packed hydrocarbon chains, the membrane thickness increases by chain stretching and the lipid area decreasing [10, 11] (Figure 2). Moreover, cholesterol can be used to modulates membrane properties at physiological temperatures, such as membrane fluidity and phase transition.

Even though it is a lipid, the molecular structure of cholesterol is quite different from that of phospholipids (as shown in Figure 1). The hydrophilic headgroup, a polar hydroxyl group, is very small. Moreover, adjacent to the hydroxyl group is a rigid plate-like steroid

structure that is composed of four fused rings. Also, there is a short single chain tail located at the ring structure.

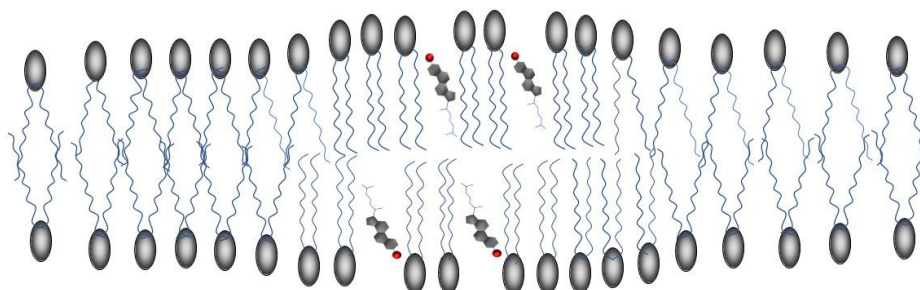


Figure 2. The schematic of membrane thickness and phospholipid hydrophobic tails alignment caused by inserted cholesterol molecules (adapted from ref. [12]). The phospholipid molecules are represented by the gray oval balls for headgroups and blue wavy lines for tails, which form a bilayer. Cholesterol molecules are represented by red spheres for hydroxyl groups, gray steroid rings, and a blue hydrophobic tail.

Cholesterol affects lipids bilayer fluidity differently at different depths. When cholesterol molecules are intercalated into the lipid bilayer, the hydroxyl group of cholesterol is surrounded by the hydrophilic phosphate headgroups, whereas the steroid ring and the short hydrocarbon chain are embedded in the lipid bilayer, alongside the acyl chains of the other lipids. As a result, the membrane fluidity increases at the bilayer headgroup region [13, 14]. This result results from increasing space among the PL induced by the presence of cholesterol in the membrane results in the increase of headgroup freedom. A computer simulation study supported this explanation [15].

Cholesterol plays a critical role in the phase transition of the bilayer. The bilayer tends to a gel state with tight packing when the temperature lowers its melting temperature. When cholesterol is added into the bilayer, the tight packing of the gel phase is disrupted by the cholesterol, and the gel phase transforms into the liquid-disordered phase (l_d) phase. This

phenomenon is called the fluidizing effect of cholesterol. The liquid-ordered phase (l_o) was found in the lipid bilayer with cholesterol molecules (as shown in Figure 3). Since cholesterol prefers to interact with saturated lipids, l_o phase (cholesterol and saturated lipid-rich domains) and l_d phases (cholesterol-poor and unsaturated lipid-rich domains) coexist in the bilayer [17]. The most remarkable difference between the l_o and l_d phases is that the saturated lipids tails are more highly ordered in the l_o phase than their counterparts in the l_d phase.

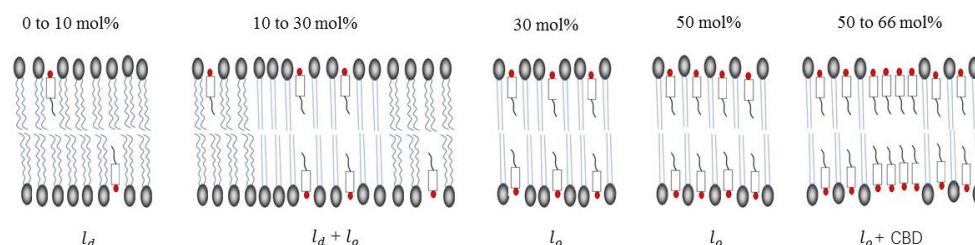


Figure 3. The schematic drawings of membrane structures formed in the DMPC/Chol mixture with different cholesterol concentrations (adapted from ref. [16]). Cholesterol molecule is represented by a red sphere for hydroxyl groups, a rectangle for steroid rings, and a gray hydrophobic tail. The DMPC is represented by the gray oval balls for headgroups and blue lines for tails. The curve lines and the straight lines represent the hydrocarbon chains in l_d phase and l_o phase, respectively. l_d , liquid-disordered phase; l_o , liquid-ordered phase; CBD, Chol bilayer domain;

1.3 The models for studying cholesterol

The nature of cholesterol-lipid interaction is a question waiting to be answered, even though lipids and cholesterol were studied a lot in membrane researches. Although some conceptual models were proposed to explain the nature of cholesterol-lipid interactions such as the Superlattice Model, Umbrella Model, and Condensed Complex Model, the fundamental molecular mechanisms of cholesterol-lipid interactions are different between these models.

The Umbrella Model was proposed to explain a crucial PL-Chol interaction: the large headgroups of PL serving as the “umbrellas” provide coverages for hydrophilic lipid tails and nonpolar bodies of the cholesterols (as shown in Figure 4). The small hydrophilic hydroxyl groups of cholesterol are not able to cover the large hydrophobic bodies of cholesterol in water. Therefore, the cholesterol molecules need the headgroups of neighboring PL to cover their hydrophilic body. Chol molecules tend to distribute in the bilayer regularly, and a cascade of “jump” in cholesterol chemical potential was predicted by this model (Figure 5b) [19].

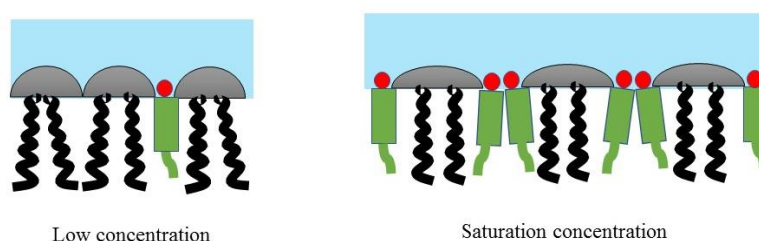


Figure 4. The umbrella model of PL and Cholesterol interaction (adapted from ref. [18]). The headgroup and hydrophilic body of cholesterol are colored in red and green, respectively. The headgroup and hydrocarbon chains of PL were represented by a gray semi-ellipse and two curve lines, respectively. The hydrophilic bodies of cholesterol are easily covered by the neighboring headgroups of PLs at a low cholesterol concentration, while the headgroups of the different PLs work together to cover the hydrophilic bodies of cholesterols at the saturation concentration.

According to Superlattice model, the difference in the cross-sectional area between cholesterol and other lipid molecules can lead to a long-range repulsive force among cholesterols and thereby produce superlattice distributions [23, 24]. The “dips” of cholesterol chemical potential are predicted by this model at the cholesterol mole fractions where superlattices occur (Figure 5a) [19, 25]. The long-range repulsive force among cholesterols plays the predominant role in cholesterol–lipid interactions in the superlattice model.

The Condensed Complex Model hypothesizes that the low free-energy stoichiometric cholesterol–lipid complexes exist and occupy smaller molecular lateral areas [18, 25]. As shown in Figure 5c, a sudden jump in cholesterol chemical potential is predicted by this model at a stoichiometric composition [22]. According to this model, the formation of cholesterol–lipid condensed complexes is a fundamental feature of cholesterol–lipid interactions.

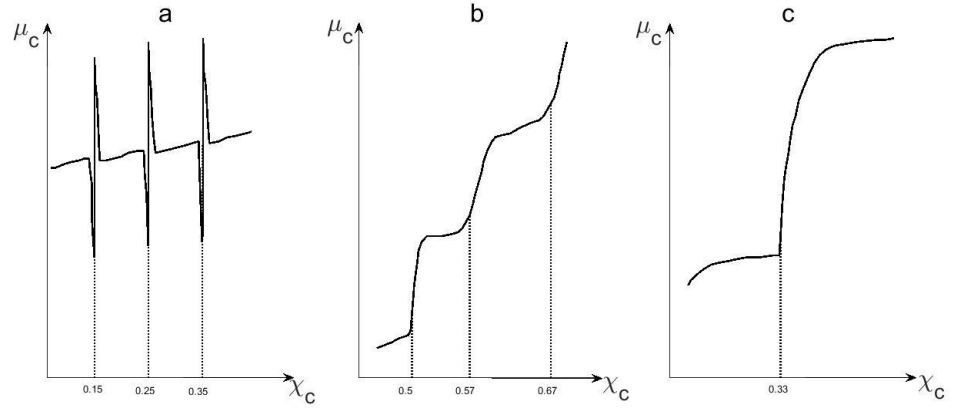


Figure 5. The schematic of the cholesterol chemical potential (μ_C) as a function of cholesterol concentration (χ_C) predicted by different models (adapted from ref. [20]). (a) The dips in free energy at superlattice compositions predicted by the Superlattice Model [21]. (b) A cascade of jump in and corresponding cholesterol regular distributions predicted by the Umbrella Model [19]. (c) A jump in at a stoichiometric composition predicted by the Condensed Complex Model [22].

The lipid bilayer with PL and Chol can be studied as a quadratic mixture in membrane thermodynamics. The lipid bilayer with two different types lipids (e.g., A and B) is a non-ideal mixture, and a quadratic mixture is the simplest non-ideal binary mixture [26-28]. The chemical potential for cholesterol in the quadratic mixture is:

$$\mu = \mu^0 + RT \ln x + h^0(1 - x)^2 \quad (1)$$

The x is number fraction (or concentration) of cholesterols. The μ^0 is the chemical potential of cholesterol in an infinitely dilute state, and $h^0 = E_{PL-Chol} - (E_{PL-PL} + E_{Chol-Chol})/2$. $E_{PL-Chol}$, E_{PL-PL} and $E_{Chol-Chol}$ are the average interaction energies for PL-Chol, PL-PL,

and Chol-Chol pairs, respectively. h^0 is unlike nearest-neighbor (i.e., PL-Chol) interaction Gibbs free energy in the mixture, and it determines whether lipids A and B mix well or separate into domains. h^0 equals to zero in an ideal mixture where random mixing occurs. If $h^0 > 0$, the mixture is nonrandom mixture where lipid A and B tend to separate into domains, and the larger h^0 is, the more complete the separation into A and B domains [29].

In quadratic mixture, cholesterol bulk/gas partition function can be determined from the following equation: the chemical potential of cholesterol in the bulk μ_b equals to its counterpart μ_g in the gas phase [30].

$$\mu_g^0 + RT \ln x_g = \mu_b^0 + RT \ln x_b + h^0(1 - x_b)^2 \quad (2)$$

$$P_{Chol} = \frac{x_b}{x_g} = P_0 e^{-h^0(1-x_b)^2/RT} \quad (3)$$

Where x_b and x_g are the concentrations of cholesterol in bulk and gas phases, respectively.

$P^0 \equiv e^{(\mu_g^0 - \mu_b^0)/RT}$ is bulk/gas partition coefficient of cholesterol in an ideal bilayer mixture where $h^0 = 0$.

According to thermodynamics, the free energy of cholesterol in bilayer can be represented by bulk/gas phase equilibrium constant. T and R are the temperature and the ideal gas constant, respectively.

$$\Delta G_{Chol} = -RT \ln K_{eq} = -RT \ln \frac{x_b}{x_g} = -RT \ln P_{Chol} \quad (4)$$

$$P_{Chol} = e^{-\Delta G_{Chol}/RT} \quad (5)$$

The following equation was determined by combining equation 3 and equation 5.

$$P_{Chol} = e^{-\Delta G_{Chol}/RT} = P_0 e^{-h^0(1-x_b)^2/RT} \quad (6)$$

According to the quadratic mixture, the lipid area in mixed bilayer can be studied by following equation [11]:

$$a(x) = a_{PL}(1 - x) + a_{Chol}x + \chi x(1 - x) \quad (7)$$

The a_{PL} and a_{Chol} are the areas of PL and cholesterol, respectively. Based on the negative or positive values of χ from fit, quadratic mixtures were subdivide with negative and positive deviation from ideal solution behavior [31]. The negative and positive χ represent the attraction and repulsion between the two species in quadratic mixtures, respectively.

According to one previous study in Grace Brannigan's lab, the free energy of Chol in POPC bilayer continuous changed along with its concentrations [30]. This is not predicted by the conceptual models (Superlattice Model, Umbrella Model, and Condensed Complex Model) but quadratic mixtures. Thus, three questions are studied in this paper. First, how well do a simple quadratic mixture model work for lateral lipid area and the free energy of cholesterol in bilayer? Secondly, how does the PL affect the free energy of cholesterol in dilute solution? Finally, does the free energy of cholesterol in bilayer depend on Chol concentration.

2 Methods

2.1 Materials

Twelve different lipids were studied in this project. They are DPPC (1,2-dipalmitoyl-sn-glycero-3-phosphocholine), DPPE (1,2-dipalmitoyl-sn-glycero-3-phosphoethanolamine), DOPC (1,2-dioleoyl-sn-glycero-3-phosphocholine), DOPE (1,2-dioleoyl-sn-glycero-3-phosphoethanolamine), DLPC (1,2-dilauroyl-sn-glycero-3-phosphocholine), DLPE (1,2-

dilauroyl-sn-glycero-3-phosphoethanolamine), SDPC (1-stearoyl-2-docosa-hexaenoyl-sn-glycero-3-phosphocholine), SDPE (1-stearoyl-2-docosa-hexaenoyl-sn-glycero-3-phosphoethanolamine), POPC (1-palmitoyl-2-oleoyl-glycero-3-phosphocholine), POPE (1-palmitoyl-2-oleoyl-glycero-3-phosphoethanolamine), PLPC (1-palmitoyl-2-linoleoyl-sn-glycero-3-phosphocholine), and PLPE (1-palmitoyl-2-linoleoyl-sn-glycero-3-phosphoethanolamine). The structures of PC lipids are shown in Figure 6.

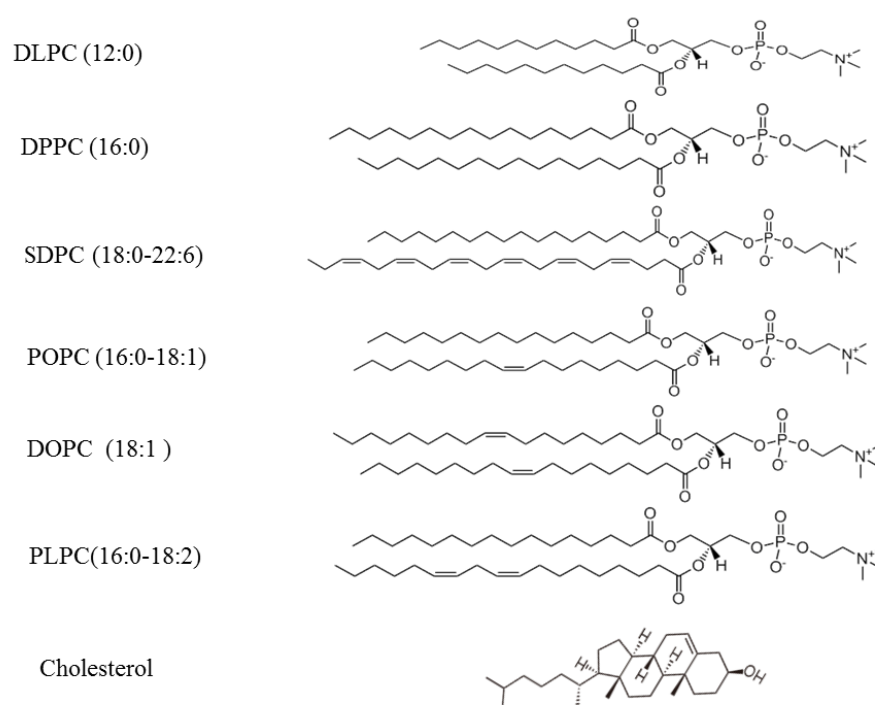


Figure 6. The structures of PC lipids and cholesterol studied in this project.

2.2 Simulation Details

Lipid-Cholesterol Mixed Bilayer System Setup.

In order to study the decoupling of a cholesterol molecule from the bulk of a lipid bilayer with various cholesterol concentrations, a series of mixed lipid/cholesterol bilayers were

generated using the CHARMM-GUI Membrane Builder [32]. Each bilayer system is composed of one type of lipid and cholesterol (mole fraction of cholesterol ranging from trace to 40%). The bilayer system was in a neutral environment with 0.15 mol/L NaCl concentration. There are 110-160 lipids (including cholesterol) molecules in the membrane for all final membrane simulation systems. Each result was the linear averaging of three replicas.

Molecular Dynamics Simulation

Before alchemical free energy perturbation calculations (AFEP), the mixing bilayer systems should be prepared by unrestrained molecular dynamics (MD) simulations. All mixed bilayer MD simulations were performed using the NAMD package (version 2.12 [33]) with Colvars Module [34], CHARMM36 force field for phospholipids [35], and modified CHARMM36 parameters [36] for cholesterol.

Each mixed bilayer system was equilibrated 100ns in the NPT ensemble at 1 atm and 300K (more details in Supplemental Table S1). The timestep is 2fs. Covalent bonds with hydrogen atoms were kept rigid using the SHAKE (non-water) or RATTLE (water) algorithms. The cutoff of electrostatic interactions was 12Å. Periodic boundary conditions were used. The long-range components were treated using the Particle Mesh Ewald (PME) method [37]. The cutoff for Lennard-Jones interactions was set to 12 Å and smoothly switched from 10 Å.

All mixed bilayer systems were energy minimized for 10 000 steps before equilibrium. The result of unrestrained mixed bilayer MD simulations were used to determine boundaries for the flat-bottom restraints in the alchemical free energy perturbation calculations. The restraints were the same as reported by Salari et al. [32].

2.3 Alchemical free energy Perturbation Calculations

The free energy of cholesterol was calculated by the AFEP. The setup of AFEP is the same as the paper written by Salari et al [30], and below description using paper text. “Decoupling via AFEP was carried using a total of 47 windows that were spaced by $\Delta\lambda = 0.05$ when $0 \leq \lambda < 0.5$, $\Delta\lambda = 0.025$ until $\lambda = 0.8$, $\Delta\lambda = 0.01$ until $\lambda = 0.95$, and $\Delta\lambda = 0.005$ until $\lambda = 1$. Simulations were performed sequentially. Each window was run for 600ps for equilibration purposes, followed by 2 ns of data collection. Thus, the total simulation time for a complete AFEP simulation was 122.2 ns. We tested convergence of the cumulative average for each window by monitoring the progression of $\langle dG \rangle$ for each λ .”

3 Results

3.1 Effect of phospholipid on condensing effect of cholesterol

The average lipid area was calculated by total lipid area divided by the total number of lipids (including PLs and Chol) in one leaflet of the bilayer. The average lipid area decreases gradually with increasing cholesterol concentration in twelve kinds of the lipid bilayer (as shown in Figure 7). This result is very similar to previous reports [11]. The lipid bilayer is condensed by cholesterol. Additionally, the ratio of lipid area change is larger in PC bilayer than PE bilayer with cholesterol concentration ranging from trace to 40%, which means that the condensing effect of cholesterol is much stronger on PC bilayer than on PE bilayer. The average lipid area is larger in PC than PE with the same hydrocarbon chains and same

cholesterol concentration, as shown in each subplot in Figure 7. The differences between PC and PE with the same hydrocarbon chains are the headgroups, and PC has a larger headgroup than that in PE (as shown in Figure 1). Thus, the larger headgroup in PC results in a larger lipid area.

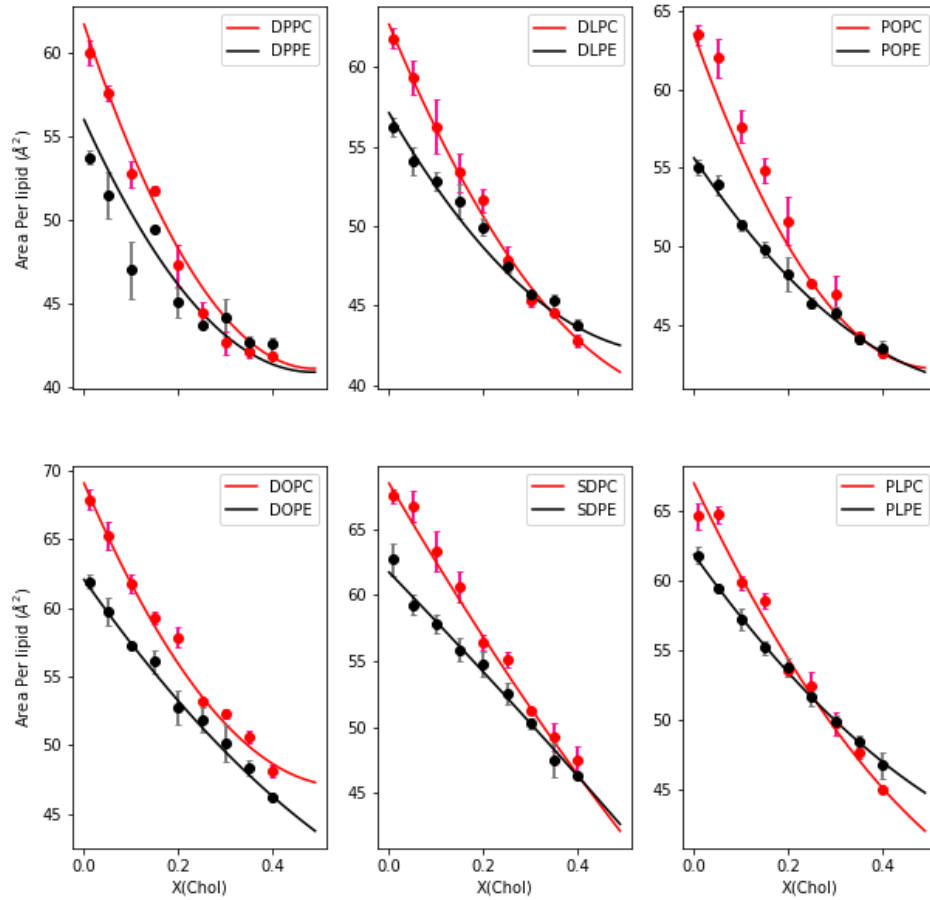


Figure 7. The average lipid area as a function of cholesterol for various PL species. Solid symbols with standard error bars show average area per lipid (with cholesterol) ($a(x)$) versus molecular fraction cholesterol (x) from 3 replicas of simulation. The solid curve shows the fit using $a(x) = a_{PL}(1 - x) + a_{Chol}x + \chi x(1 - x)$. The red and black curves in each subplot represent PC and PE lipids, respectively.

The χ values in Figure 8 derived from the curve fitting of the average lipid area along with the Chol concentration in Figure 7. The negative χ value means that mixed bilayer is a negative deviation from the ideal solution, and also means the attractive interaction between

PL and cholesterol. The absolute values of χ are larger in PC bilayers than in PE bilayers, which indicates the attraction of PC-Chol is much stronger than the attraction of PE-Chol. This result is consistent with the previous finding that the condensing effect of cholesterol is much stronger on PC than on PE. Furthermore, the differences between the molecular pairs are their headgroups, and the order of the headgroups size is PC > PE >> Chol (as shown in Figure 1). Therefore, comparing to PE lipids, the larger headgroup of PC leads to the stronger attraction between PC and Chol.

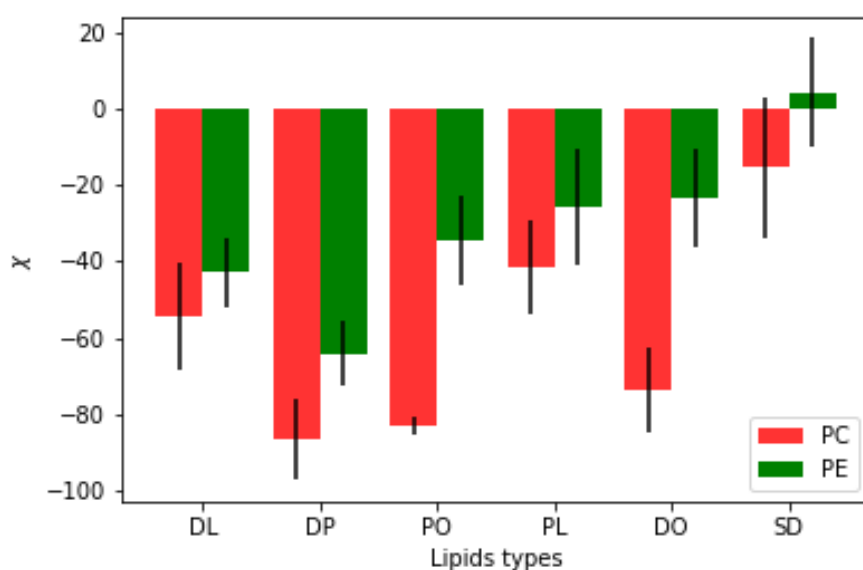


Figure 8. The attractive interaction between Chol and PL. The χ values come from the data fitting in Figure 7.

3.2 Effect of phospholipid on chemical potential of dilute cholesterol

The free energy of cholesterol in the bilayer with dilute cholesterol was calculated using AFEP by decoupling a cholesterol molecule from the bilayer in MD simulation. The free energy

of cholesterol is higher in PC bilayer than in PE bilayer, as shown in Figure 9. This result agrees with the above result that the attraction of PC-Chol is much stronger than the attraction of PE-Chol. The headgroup of PL is the only difference between PC bilayer and PE bilayer with the same hydrocarbon chains. Thus, the larger headgroup in PC lipid results in the higher free energy of cholesterol in PC bilayer.

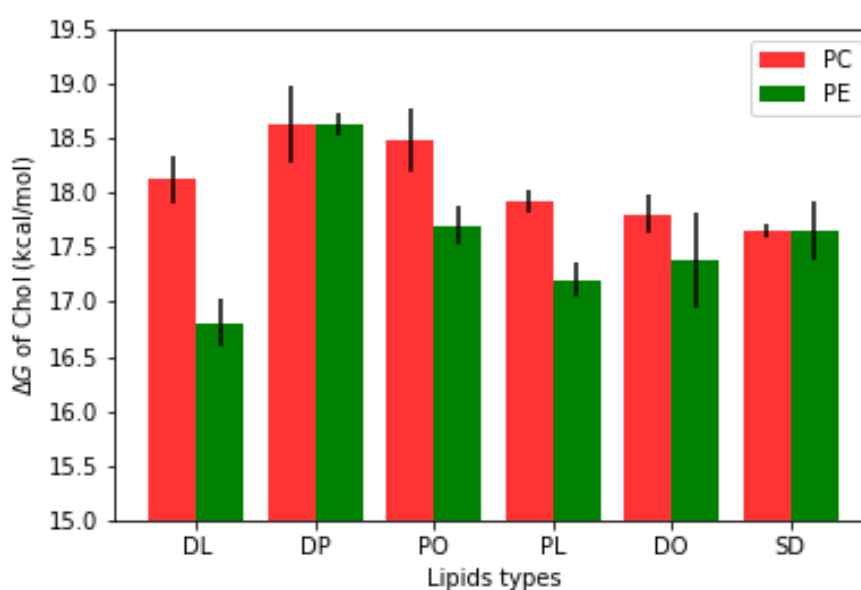


Figure 9. The free energy of removing a single cholesterol molecule from mixed lipid bilayer with dilute cholesterol at 300K. The higher free energy of cholesterol, the more favorable for the cholesterol to stay at the membrane.

For saturated PL bilayers, the free energy of cholesterol is higher in DPPC bilayer than in DLPC bilayer. Similarly, cholesterol has higher free energy in DPPE bilayer than in DLPE bilayer. This result is in line with a previous result that the absolute values of χ are larger in DPPC (or DLPC) bilayers than their counterparts in DPPE (or DLPE) bilayers (Figure 8). It seems that the longer saturated hydrocarbon chains in DPPC (or DPPE) lead to the higher free energy of cholesterol.

For unsaturated PL bilayers, the free energy of cholesterol decreases in some bilayers, and the order is DPPC, POPC, PLPC (or DOPC). Since the hydrocarbon chains length in these PL (DPPC, POPC, PLPC, and DOPC) are very close (16 or 18), the predominant difference between these PLs is the degree of unsaturation of hydrocarbon chains. The unsaturated degree of DPPC, POPC, and PLPC (or DOPC) are 0, 1, and 2 (or 2), respectively (Figure 6). Similarly, this finding occurs in the PE lipid (DPPE, POPE, and PLPE (or DOPE)). It seems that the decreasing of free energy of cholesterol in the bilayer of DPPC, POPC, PLPC (DOPC) results from the increasing of the unsaturation degree in these lipids.

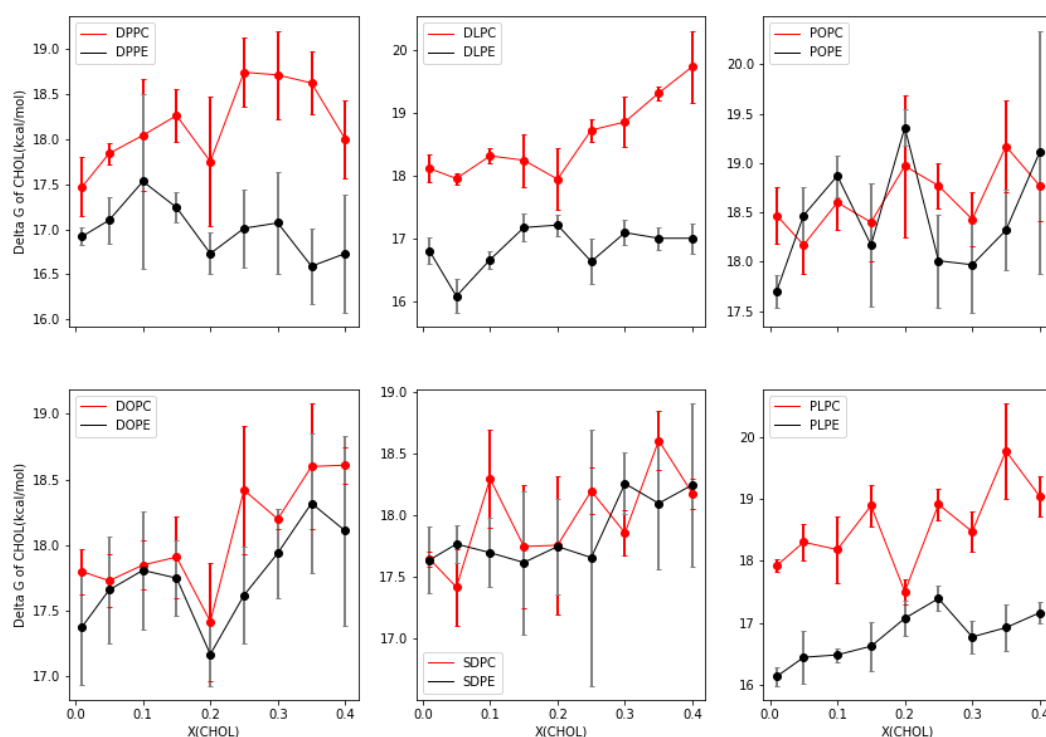


Figure 10. The free energy of cholesterol in different bilayers with varied cholesterol concentration. The two lines in each subplot represent the two types lipids with the same hydrophobic tails and different hydrophilic head groups (PC and PE). The POPC data comes from the ref. [30].

3.3 Effect of phospholipid on cholesterol non-ideality

In non-ideal mixed bilayers, the free energy of cholesterol in bilayer was calculated using AFEP by decoupling a cholesterol molecule from the bilayer with varied cholesterol concentrations. For a series of bilayers with the same PL and with different cholesterol concentrations, the free energy of cholesterol in bilayers is changeable, and the amplitude of variation is relatively small, as shown in Figure 10. The change tendency of the free energy of cholesterol along its concentrations is diverse for all bilayers. However, a few “dips” occur in the most bilayers, such as DOPC, DOPE, and PLPC. The free energy of cholesterol changes a lot around the dips.

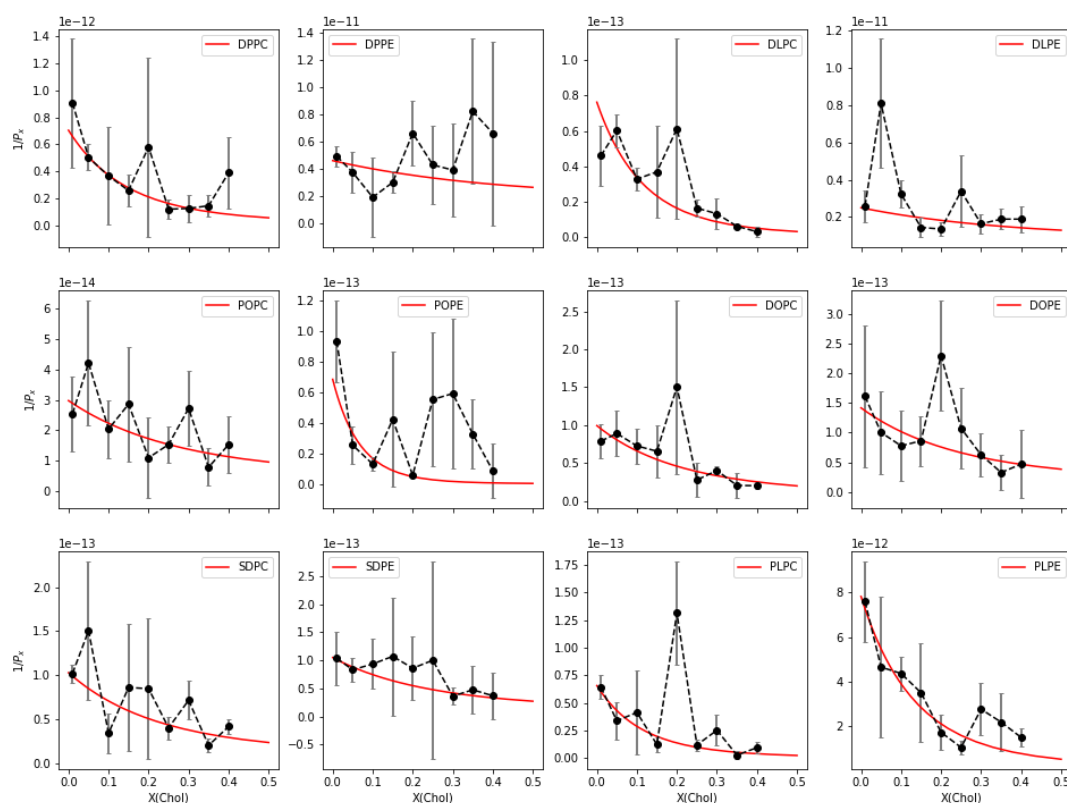


Figure 11. The effect of cholesterol fraction on the inverse gas/bulk partition coefficient $1/P_x$, as calculated by AFEP decoupling of a single cholesterol molecule from mixed lipids bilayer with Chol.

Black points with standard error bars represent the average of three replicas. The curve represents the fit function ($\frac{1}{p_x} = \frac{1}{p^0} \exp[h^0(1 - x_{CHOL})^2 / RT]$).

The interactions (h^0) between Chol and PL in Figure 12 come from the fit function in Figure 11. First, the h^0 values are nonzero in twelve bilayer mixtures, which indicates that these mixed bilayers are non-ideal because the h^0 equals to zero in the ideal mixture. Moreover, the positive h^0 indicates the attractive interaction between Chol and PL, and the pair interactions energy between Chol and PC are higher than Chol and PC interactions. These results agree with the χ values in Figure 8.

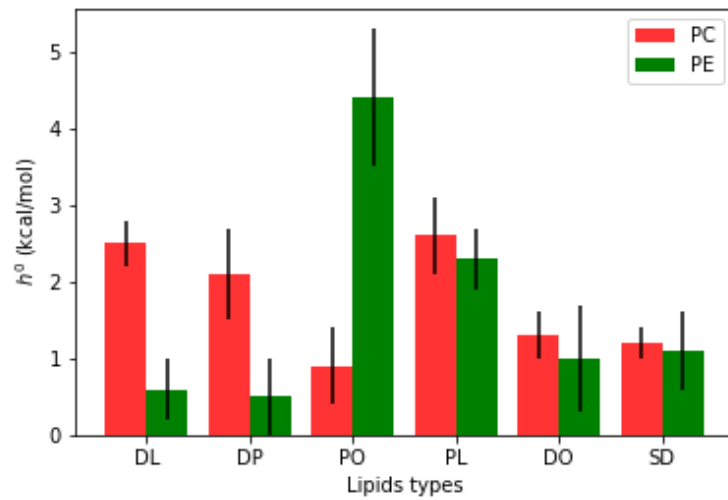


Figure 12. The h^0 in the different lipid bilayers. The values of h^0 come from the fit in Figure 11.

4 Discussion

In this research, the condensing effect of cholesterol on lipid bilayer was observed in twelve bilayers by the calculation of lipid lateral area on the bilayer. The result is very similar to previous reports [12]. Besides, the negative χ indicates the attractive interaction between cholesterol and PL, and the larger headgroup of PL results in a stronger attraction between Chol

and PL. Since the results from twelve bilayers are similar, the quadratic mixture model works well for lateral lipid area.

One finding is that the condensing effect of cholesterol is more distinct on PC bilayer than that on PE bilayer. According to Umbrella Model, the larger headgroup in PC provide a bigger cover to keep the hydrocarbon chains from exposure to water. It leads to the loose lipid packing in lateral distribution. Furthermore, the strong attraction between PC and Chol can be the force to condense the bilayer. Thus, the condensing effect of cholesterol is very obvious in PC bilayer with loose lipid packing.

In bilayer mixtures with infinitely dilute cholesterol, the larger headgroups in the PC, compared to PE, result in the higher free energy of cholesterol in the bilayer. This result is consistent with the attractive interaction of Chol-PL where the attraction is much stronger in PC-Chol than in PE-Chol. Furthermore, the longer saturated hydrocarbon chains lead to the increasing free energy of cholesterol in the bilayer. However, the unsaturated lipid decreases the free energy of cholesterol in PL bilayers. These results indicate that cholesterol prefers to stay with saturated lipids than unsaturated lipids. It happens in coexist phases- L_o phase (cholesterol and saturated lipid-rich domains) and L_d phases (cholesterol-poor and unsaturated lipid rich domains) [17].

In non-ideal bilayer mixture, the free energy of cholesterol in the bilayer is changeable with its concentrations, and it is hard to find a general rule to summarize the changes in all bilayer. Some reasons may lead to this result. For one thing, the random error may occur in AFEP. Some data in Figure 10 have large standard errors. The AFEP focus on one cholesterol

molecule. Moreover, cholesterol has different free energy in different phases. Three possible phases (l_d phase, $l_d + l_o$ phases, and l_o phase) occur in lipid bilayers at multiple cholesterol concentration ranging from trace to 40%, as shown in Figure 2. Furthermore, in the bilayer with dilute cholesterol, cholesterol is surrounded by PLs in bilayer where the Chol-Chol interactions can be ignored in statistics. Nevertheless, Chol-Chol interactions can not be neglected in non-dilute cholesterol mixture, and it can affect cholesterol free energy in the bilayer. Thus, the free energy of cholesterol is not constant in the bilayer with various cholesterol concentration.

According to quadratic mixtures (liquid), the cholesterol free energy should continuously change along with its concentration. But some dips occur in Figure 10. It seems that quadratic mixture does not work well for the free energy of cholesterol in lipid bilayers. It seems that the dips in the free energy of cholesterol in lipid bilayers support the superlattice model. However, more data need to be done to confirm it. According to the superlattice model, the cholesterol regularly distributes at the “dips” points. The cholesterol radial distribution is another to confirm the dips. Moreover, more sampling around the dips should be studied.

5 References

1. Andersen, O. S. & Koeppe, R. E. Bilayer Thickness and Membrane Protein Function: An Energetic Perspective. *Annu. Rev. Biophys. Biomol. Struct.* **36**, 107–130 (2007).
2. Meer, G. Van, Voelker, D. R. & Feigenson, G. W. Membrane lipids : where they are and how they behave. **9**, (2008).
3. Silverstein, T. P. The Real Reason Why Oil and Water Don't Mix. *J. Chem. Educ.* **75**, 116 (2009).
4. Gennis, R. B. Introduction: The Structure and Composition of Biomembranes. 1–35 (2013). doi:10.1007/978-1-4757-2065-5_1
5. Berg, H. C. Random Walks Ch1. *Molecules* 2–8 (1998).
6. Soos, I. Beiträge zur Gasanalyse. V Weitere Anwendungen des Druckverfahrens. *Zeitschrift für Anal. Chemie* **127**, 188–191 (1944).
7. Dawaliby, R. *et al.* Phosphatidylethanolamine is a key regulator of membrane fluidity in eukaryotic cells. *J. Biol. Chem.* **291**, 3658–3667 (2016).
8. Subczynski, W. K., Justyna, M. P., Mainali, L. & Raguz, M. High Cholesterol / Low Cholesterol : Effects in Biological Membranes : A Review. *Cell Biochem. Biophys.* 369–385 (2017). doi:10.1007/s12013-017-0792-7
9. Edholm, O. & Nagle, J. F. Areas of molecules in membranes consisting of mixtures. *Biophys. J.* **89**, 1827–1832 (2005).
10. Pan, D., Wang, W., Liu, W., Yang, L. & Huang, H. W. Chain packing in the inverted hexagonal phase of phospholipids: A study by X-ray anomalous diffraction on bromine-labeled chains. *J. Am. Chem. Soc.* **128**, 3800–3807 (2006).
11. Hung, W., Lee, M., Chen, F. & Huang, H. W. The Condensing Effect of Cholesterol in Lipid Bilayers. **92**, 3960–3967 (2007).
12. Ayee, M. A. & Levitan, I. Paradoxical impact of cholesterol on lipid packing and cell stiffness. *Front. Biosci. - Landmark* **21**, 1245–1259 (2016).
13. Mainali, L., Feix, J. B., Hyde, J. S. & Subczynski, W. K. Membrane fluidity profiles as deduced by saturation-recovery EPR measurements of spin-lattice relaxation times of spin labels. *J. Magn. Reson.* **212**, 418–425 (2011).
14. Mainali, L., Hyde, J. S. & Subczynski, W. K. Using spin-label W-band EPR to study membrane fluidity profiles in samples of small volume. *J. Magn. Reson.* **226**, 35–44 (2013).
15. Murzyn, K., Róg, T., Grzegorz, J., Takaoka, Y. & Pasenkiewicz-Gierula, M. Effects of Phospholipid Unsaturation on the Membrane / Water Interface : *Biophys. J.* **81**, 170–183 (2001).
16. Mainali, L., Raguz, M. & Subczynski, W. K. Formation of cholesterol bilayer domains precedes formation of cholesterol crystals in cholesterol/dimyristoylphosphatidylcholine membranes: EPR and DSC studies. *J. Phys. Chem. B* **117**, 8994–9003 (2013).

17. Davis, J. H., Clair, J. J. & Juhasz, J. Phase Equilibria in DOPC / DPPC-d 62 / Cholesterol Mixtures. *Biophysj* **96**, 521–539 (2009).
18. McConnell, H. M. & Radhakrishnan, A. Condensed complexes of cholesterol and phospholipids. *Biochim. Biophys. Acta - Biomembr.* **1610**, 159–173 (2003).
19. Huang, J. & Feigenson, G. W. A microscopic interaction model of maximum solubility of cholesterol in lipid bilayers. *Biophys. J.* **76**, 2142–2157 (1999).
20. Ali, R., Cheng, K. H. & Huang, J. Assess the nature of cholesterol – lipid interactions through the chemical potential of cholesterol in phosphatidylcholine bilayers. **104**, 5372–5377 (2007).
21. Somerharju, P., Virtanen, J. A., Cheng, K. H. & Hermansson, M. The superlattice model of lateral organization of membranes and its implications on membrane lipid homeostasis. *Biochim. Biophys. Acta - Biomembr.* **1788**, 12–23 (2009).
22. Radhakrishnan, A. & McConnell, H. M. Chemical activity of cholesterol in membranes. *Biochemistry* **39**, 8119–8124 (2000).
23. Chong, P. L. Evidence for regular distribution of sterols in liquid crystalline phosphatidylcholine bilayers. *Proc. Natl. Acad. Sci.* **91**, 10069–10073 (1994).
24. Koivusalo, M., Alvesalo, J., Virtanen, J. A. & Somerharju, P. Partitioning of Pyrene-Labeled Phospho- and Sphingolipids between Ordered and Disordered Bilayer Domains. *Biophys. J.* **86**, 923–935 (2004).
25. Radhakrishnan, A., Anderson, T. G. & McConnell, H. M. Condensed complexes, rafts, and the chemical activity of cholesterol in membranes. *Proc. Natl. Acad. Sci.* **97**, 12422–12427 (2000).
26. Rowlinson, J. S. & Swinton, F. L. Liquids and Liquid Mixtures: Butterworths Monographs in Chemistry. 336 (1982).
27. Spiegel-Adolf, M. *Physical chemistry of lipoids.* *Biochemical Journal* **30**, (1936).
28. Thermodynamics, W. S. *et al.* Chapter 1 : Introduction. 1–20
29. Almeida, P. F. F., Pokorny, A. & Hinderliter, A. Thermodynamics of membrane domains. *Biochim. Biophys. Acta - Biomembr.* **1720**, 1–13 (2005).
30. Brannigan, G. A Streamlined, General Approach for Computing Ligand Binding Free Energies and Its Application to GPCR-Bound Cholesterol. (2018). doi:10.1021/acs.jctc.8b00447
31. Durov, V. A. Models of liquid mixtures: Structure, dynamics, and properties. *Pure Appl. Chem.* **76**, 1–10 (2007).
32. Szalay, F. I. A. Fast Calculation of DNMR Spectra on CUDA-Enabled Graphics Card. *J. Comput. Chem.* (2010). doi:10.1002/jcc
33. Phillips, J. C. *et al.* Scalable molecular dynamics with \uppercase{NAMD}. *J. Comput. Chem.* **26**, 1781–1802 (2005).
34. Fiorin, G., Klein, M. L. & Hénin, J. Using collective variables to drive molecular dynamics simulations. *Mol. Phys.* **111**, 3345–3362 (2013).
35. Klauda, J. B. *et al.* Update of the CHARMM All-Atom Additive Force Field for Lipids: Validation on Six Lipid Types. *J. Phys. Chem. B* **114**, 7830–7843 (2010).

36. Lim, J. B., Rogaski, B. & Klauda, J. B. Update of the cholesterol force field parameters in CHARMM. *J. Phys. Chem. B* **116**, 203–210 (2012).
37. Ulrich, E. *et al.* A smooth particle mesh Ewald method. *J. Chem. Phys.* **103**, 8577–8593 (1995).

6 Supplemental Material

Table S1: Lipids areas and fitted parameters χ of bilayer (coming from Figure 7).

Lipid bilayers	Simulation Temperature (K)	χ	χ error value	lipids Area in simulation a_{PL} (\AA^2)
DPPC	320	-86.5	10.6	61.7
DPPE	330	-64.1	8.5	56
DLPC	300	-54.4	14	62.7
DLPE	320	-42.9	8.9	57.1
POPC	300	-82.8	2.3	63.5
POPE	300	-34.5	11.8	55.6
DOPC	300	-73.5	11.2	69.1
DOPE	300	-23.5	12.8	62.1
SDPC	300	-15.5	18.5	68.5
SDPE	300	4.1	14.2	61.7
PLPC	300	-41.8	12.3	67
PLPE	320	-25.6	15.1	61.9

Table S2. The P^0 and h^0 of the cholesterol in the different lipid bilayers. The values of P^0 and h^0 come from the fit in Figure 11.

Simulation system	Simulation Temperature/K	P^0	h^0	h^0 error value
DPPC	320	4.10×10^{13}	2.1	0.6
DPPE	330	4.50×10^{11}	0.5	0.5
DLPC	300	9.70×10^{14}	2.5	0.3
DLPE	320	9.70×10^{11}	0.6	0.4
POPC	300	1.50×10^{14}	0.9	0.5
POPE	300	2.50×10^{16}	4.4	0.9
DOPC	300	8.70×10^{13}	1.3	0.3
DOPE	300	4.00×10^{13}	1	0.7
SDPC	300	7.00×10^{13}	1.2	0.2
SDPE	300	5.80×10^{13}	1.1	0.5
PLPC	300	1.20×10^{15}	2.6	0.5
PLPE	320	5.00×10^{12}	2.3	0.4